Electronic Supplementary Material (ESI) for Journal of Materials Chemistry A.
This journal is © The Royal Society of Chemistry 2019

A Quasi-Solid-State Photothermal Supercapacitor via Enhanced Solar Energy Harvest

Mingyu Zhao[1,3], Yaling Li[1], Feng Lin[1], Yunshi Xu[1], Leilei Chen[1,2], Weicun Jiang[1], Ting Jiang[1,2], Shuguang Yang[1] and Yi Wang[1,2,]*

[1]Chemical Fibers and Polymer Materials, College of Materials Science and Engineering, Donghua University, Shanghai 201620, China

[2]College of Chemistry, Chemical Engineering and Biotechnology, Donghua University, Shanghai 201620, China

[3]Current address: Department of Mechanical Engineering, The University of Texas at Austin, Austin, TX 78712, USA

[*]E-mail: ywang@dhu.edu.cn

KEYWORDS: photothermal supercapacitors, solar energy, mesoporous carbon nanospheres, graphene hydrogel, flexibility

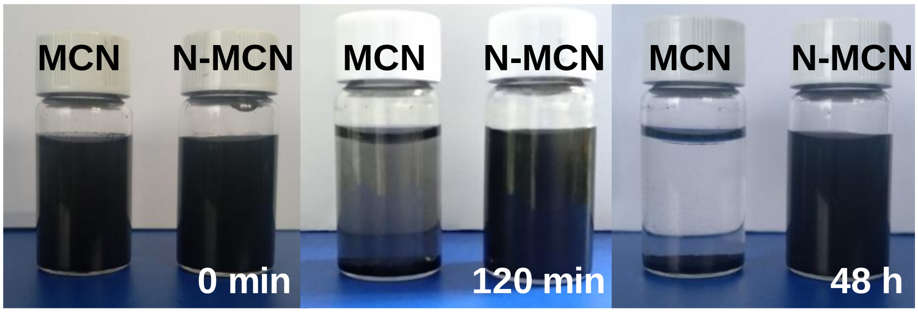

Figure S1. Digital photographs of MCN and N-MCN aqueous solution after standing for different time periods. It showed that N-MCN had enhanced water-dispersity and hydrophilicity/wettability.

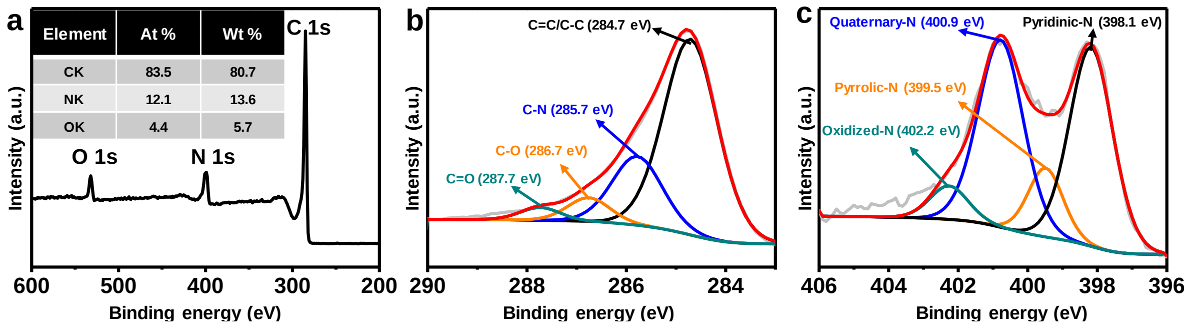

Figure S2. (a) XPS survey spectra, (b, c) C 1s and N 1s spectra of N-MCN. It showed that the N with the dominated Pyridinic-N and Quaternary-N was doped into MCN with plentiful sp2-hybrided carbon framework.

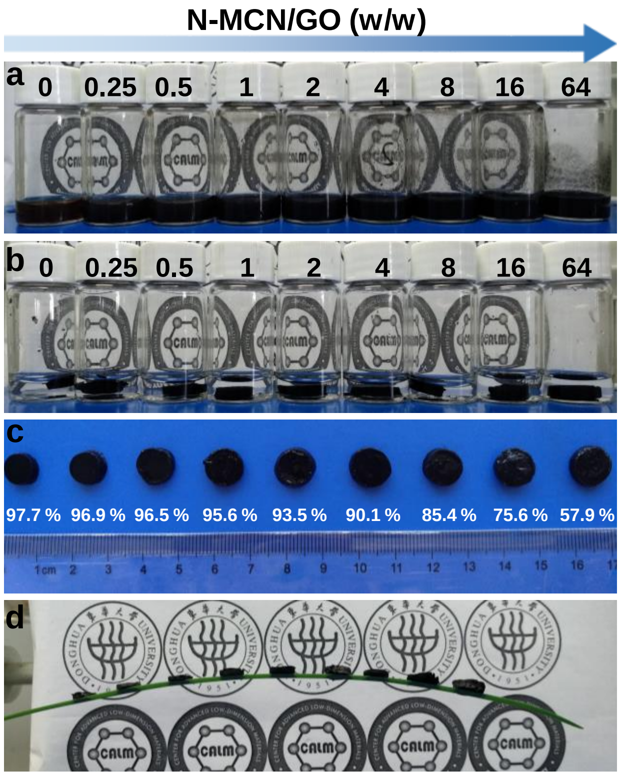

Figure S3. Digital photographs for the facile formation of N-MCN@GH hydrogels and aerogels under a wide N-MCN/GO ratios: (a) N-MCN/GO solution. (b) After hydrothermal treatment. (c) N-MCN@GH hydrogels with various water contents. (c) Light-weight N-MCN@GH aerogels obtained via freeze drying.

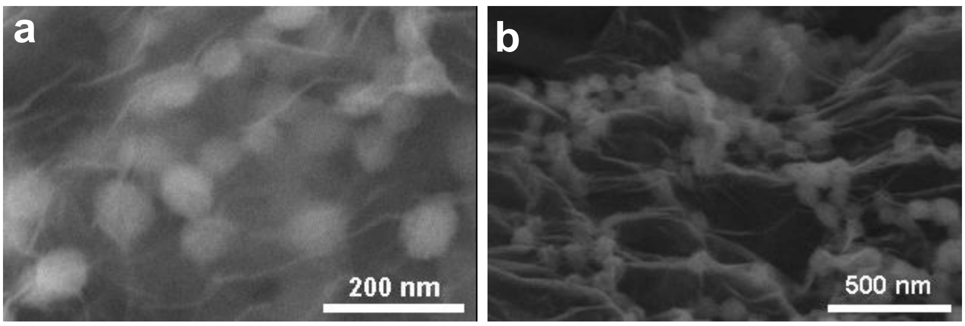

Figure S4. SEM images of N-MCN@GH. It showed that the dispersed N-MCN was homogeneously intercalated between graphene nanosheets to build a 3D porous architecture.

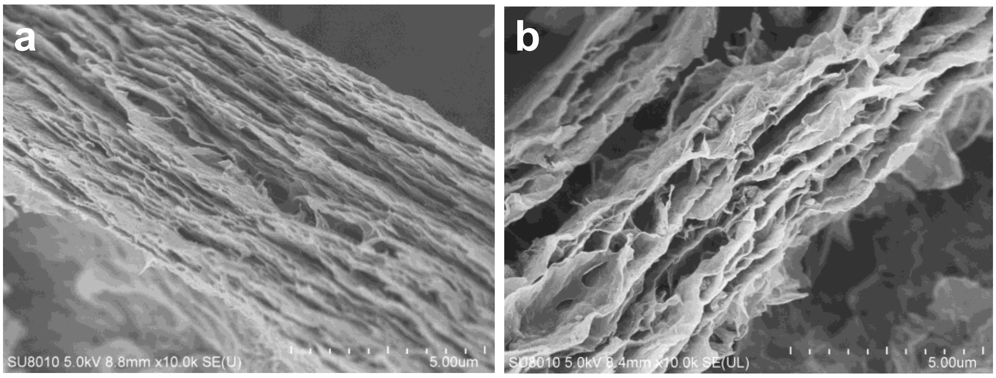

Figure S5. Cross section-view SEM images of (a) GH and (b) N-MCN@GH films. The enlarged interlayer spacing of N-MCN@GH revealed the intercalation of N-MCN between graphene nanosheets.

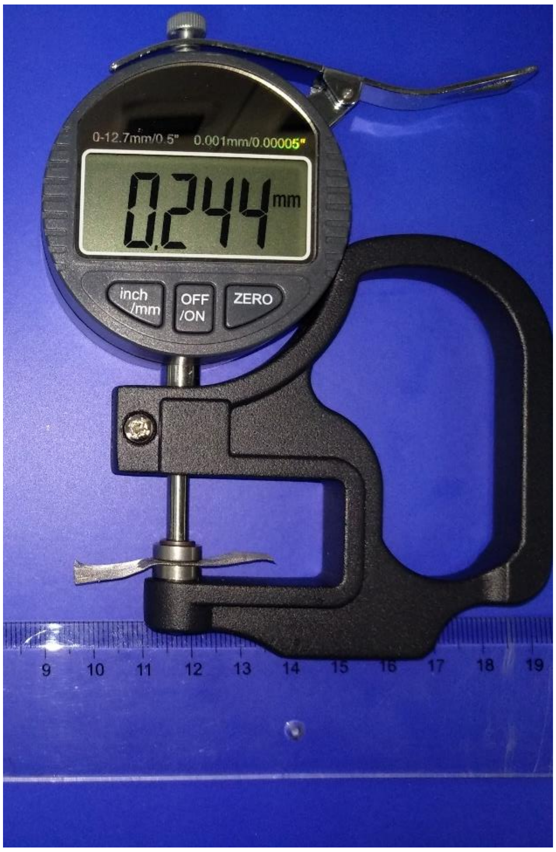

Figure S6. Photographs of a flexible supercapacitor based on N-MCN@GH film electrode and its compact configuration, with a thickness of 0.25 mm.

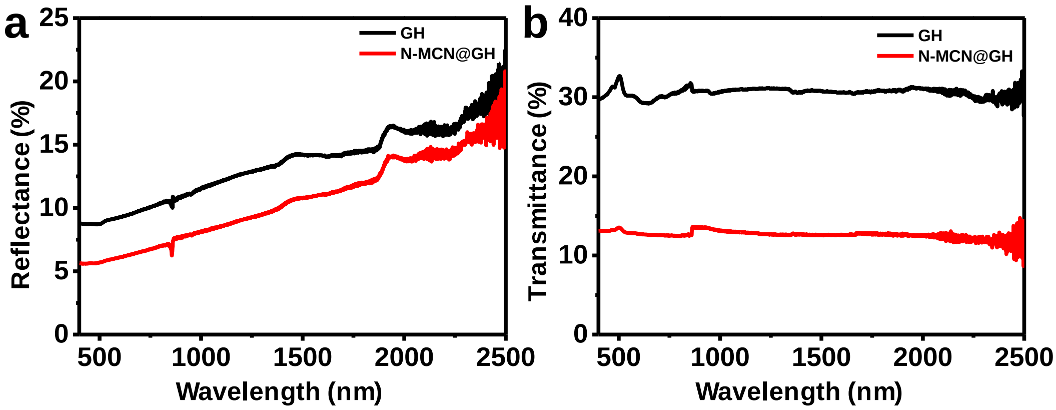

Figure S7. (a) Reflection spectra and (b) Transmission spectra of the GH and N-MCN@GH films. N-MCN@GH had lower reflection and transmission than GH, suggesting the N-MCN intercalation-produced 3D hierarchical porous network for multiple scattering with high absorption.

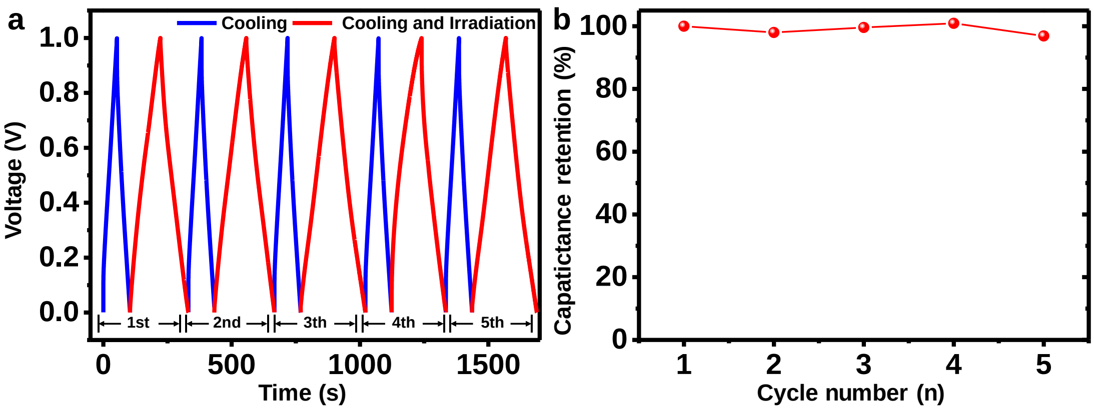

Figure S8. (a) The cycled GCD curves at a current density of 1 A g^{-1}, where blue lines represented the cooling to the 5 °C and red lines represented the cooling and irradiation for 10 min. (b) Capacitance retention of N-MCN@GH supercapacitor after different cooling and irradiation cycles as illustrated in “a”.

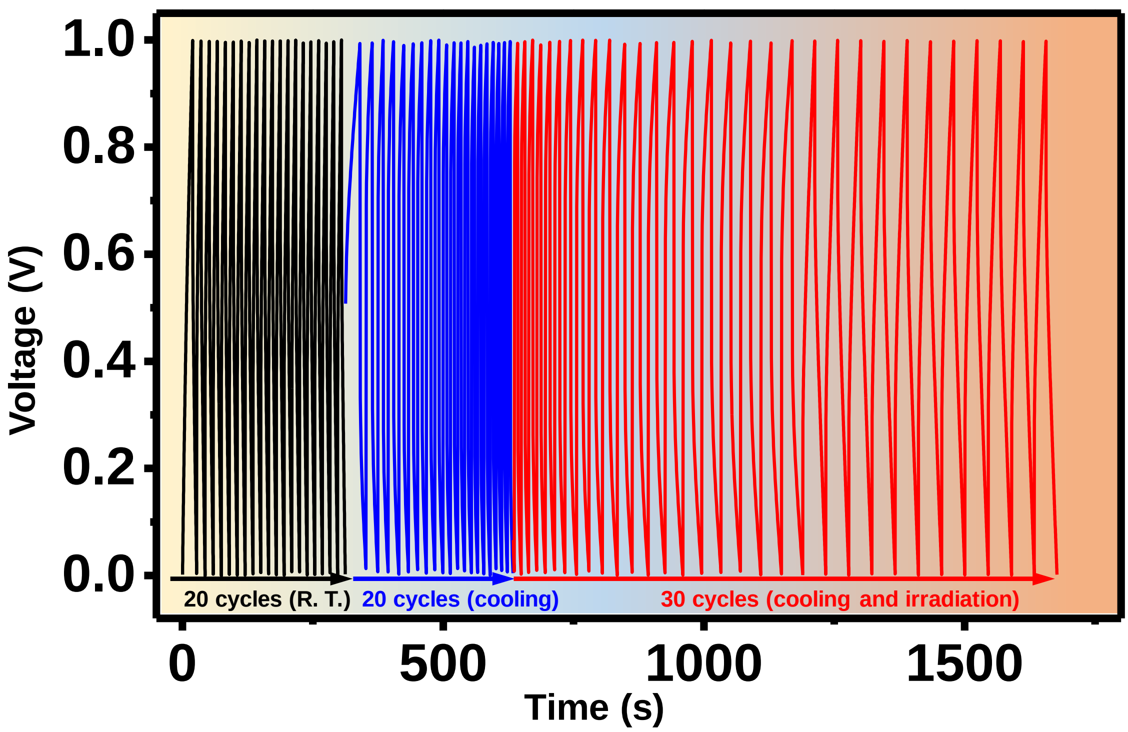

Figure S9. Galvanostatic charge/discharge curves of N-MCN@GH at a current density of 5 A g^{-1} under different environmental conditions.

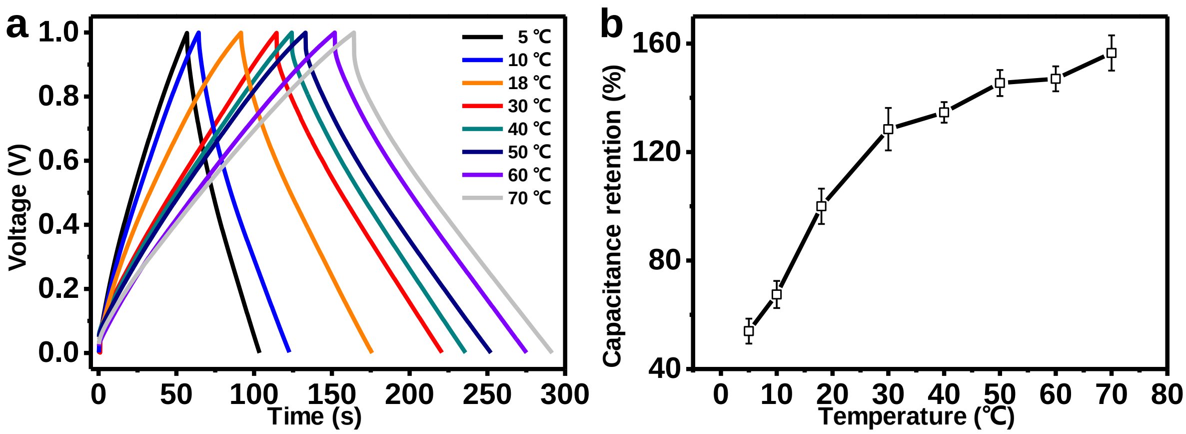

Figure S10. (a) GCD curves at a current density of 1 A g^{-1} and (b) corresponding capacitance curve of N-MCN@GH supercapacitor at different environment temperatures.

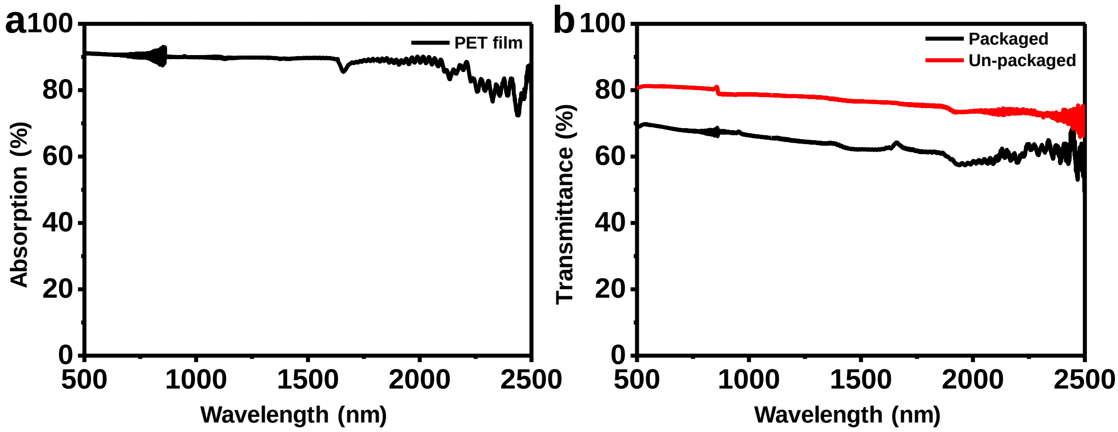

Figure S11. (a) Transmission spectra of the PET films. (b) UV-vis-NIR absorption spectra of N-MCN@GH electrodes with/without PET film packaged.

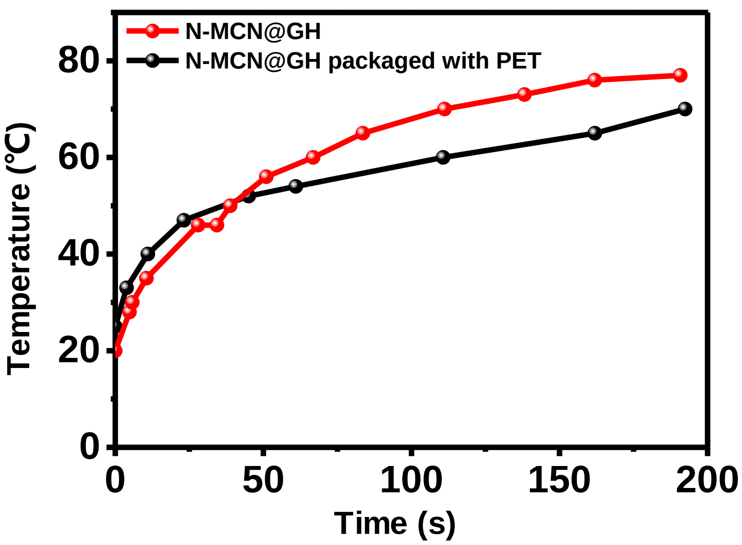

Figure S12. Solar-thermal heating curves N-MCN@GH electrodes with/without PET film packaged under the simulated sunlight illumination (0.36 W/cm^{-2}).

Table S1.
Structural properties of the GH and N-MCN@GH.

Sample	BET surface area (m^2 g^{-1})	Pore volume (cm^3 g^{-1})	Micropore volume (cm^3 g^{-1})	t-Plot Micropore Area (m^2 g^{-1})	Mesopore volume (cm^3 g^{-1})
GH	125	0.53	0.03	62.67	0.52
N-MCN@GH	742	1.19	0.10	187.11	1.11

Table S2.
Comparisons of the electrochemical performance of N-MCN@GH with the reported flexible supercapacitors.

Active material	Electrolyte	Potential window	Volumetric Capacitance	Capacitance retention/ cycle number	Energy density (mWh cm^{-3})	Power density (mW cm^{-3})	Ref.
Laser Scribing graphene	PVA/H_3PO_4	1 V	3.67 mF cm^{-2}	96.5%/10000	1.36	200	*Science* **2012**, 335, 1326-1330
Fe_2O_3/PPy	PVA/LiCl	1.6 V	382.4 mF cm^{-2} at 0.5 mAcm^{-2}	97%/5000	0.22	165.6	*Angew. Chem., Int. Ed.* **2017**, 56, 1105.
Ni/MnO_2	PVA/Na_2SO_4	2.5 V	1.4 F cm^{-3} at 2.5 mA cm^{-3}	85%/1000	0.78	2.5	*ACS Nano* **2016**, 10, 1273.
MnO_2@NNA//Ppy@NNA	Na_2SO_4	1.6 V	135.15 mF cm^{-2} at 3 A g^{-1}	106%/20000	1.23	310	*Adv. Mater.* **2016**, 28, 4105.
rGO/Fe_2O_3	PVA/KOH	1 V	0.25 F cm^{-3}	96%/5000	0.035	0.003	*Chemistry of Materials* **2017**, 29,14: 6058-65.
Ni-Mn-C	PVA/KOH	0.6 V	0.53 F cm^{-3}	86%/10000	0.027	36.20	*J. Mater. Chem. A* **2018**, 6,47: 24086-91.
MnO_2	PVA/LiCl	0.8 V	2 F cm^{-3} at 0.5A g^{-1}	91%/20000	0.17	1	*Nanoscale* **2017**,9,3593-3600
Graphene	PVA/H_2SO_4	1 V	4.21mF cm^{-2} at 0.41mA cm^{-2}	95%/10000	0.552	561.9	*ACS Appl. Mater. Interfaces* **2017**, 9, 9763−9771
N-MCN@GH	PVA/H_2SO_4	1 V	8.1F cm^{-3} 197.5 mF cm^{-2} at 0.64 mA cm^{-2}	80%/10000	1.12	522.08	This work